The 2013 World Congress on
Advances in Structural Engineering and Mechanics (ASEM13)
Jeju, Korea, September 8-12, 2013

LQG design scheme for multiple vibration controllers in a building–equipment system considering the maximum control force

*Masayuki Kohiyama[1)] and Minako Yoshida[2)]

[1), 2)] *Graduate School of Science and Technology, Keio University, Yokohama 223-8522, Japan*
[1)] *kohiyama@sd.keio.ac.jp*

ABSTRACT

A method to determine a control scheme and parameters is proposed for a data center facility with a vibration controller on its top floor and a secondary isolation device with its own vibration controller designed to protect delicate computer equipment. The aim is to reduce acceleration and drift from an earthquake for computer servers placed on the isolation device that must operate during a seismic event. A linear elastic model was constructed and the evaluation function of the linear quadratic Gaussian control was formulated. The relationship between control parameters and responses was examined, and it was confirmed that the proposed scheme properly defined system parameters to minimize the responses of both the building and computer server.

1. INTRODUCTION

Data center facilities are expected to operate uninterrupted, even during a severe earthquake (Japan Data Center Council 2012). To achieve this, server computers are often set up on an isolation table or floor. Such isolation devices dampen the acceleration due to an earthquake for the servers placed on them. However, if the drift experienced on the isolation device is larger than its allowable limit, the servers can fall or collide with other objects and cause damage that would interrupt their functionality. To prevent this, a vibration control device can be used to reduce the drift of an isolation device.

This paper proposes a method to determine a control scheme and to design parameters of a linear quadratic Gaussian (LQG) controller considering the maximum control force and the relationship between control parameters and responses. This method can improve functional continuity and operability of servers during and after an earthquake. Specifically, this paper focuses on a building that has a vibration controller

[1)] Associate Professor
[2)] Former Graduate Student

on the top floor and a server on an isolation device with a semi-active oil damper working as a second vibration controller.

2. MODELING OF A TARGET SYSTEM

The building under investigation has an active mass damper (AMD) installed on the top floor, which accommodates a server computer placed on an isolation device with a semi-active oil damper. A linear elastic response of the system is assumed. The equation of motion is given as follows:

$$\mathbf{M}\ddot{\mathbf{x}}_{\mathrm{c}}(t) + \mathbf{C}\dot{\mathbf{x}}_{\mathrm{c}}(t) + \mathbf{K}\mathbf{x}_{\mathrm{c}}(t) = -\mathbf{M}\{1\}\ddot{z}(t) + \mathbf{f}\mathbf{u}(t) \tag{1}$$

where **M**, **C**, and **K** are the mass, damping, and stiffness matrices, respectively. The vectors $\mathbf{x}_{\mathrm{c}}$, **u**, and **f** denote the displacement of the system, the control forces of the AMD and semi-active oil damper, and the location to apply the control forces, respectively. The variable *z* represents the ground displacement.

Using the equation of motion, the system equations are given as follows:

$$\dot{\mathbf{x}}(t) = \mathbf{A}\mathbf{x}(t) + \mathbf{B}\mathbf{u}(t) + \mathbf{G}\,\ddot{z}(t) \tag{2}$$

$$\mathbf{u}(t) = -\mathbf{F}_{\mathrm{ctrl}}\hat{\mathbf{x}}(t) \tag{3}$$

$$\dot{\hat{\mathbf{x}}}(t) = \mathbf{A}\hat{\mathbf{x}}(t) + \mathbf{B}\mathbf{u}(t) + \mathbf{F}_{\mathrm{obs}}\left(\mathbf{y}_{\mathrm{obs}}(t) - \hat{\mathbf{y}}_{\mathrm{obs}}(t)\right) \tag{4}$$

$$\mathbf{y}_{\mathrm{obs}}(t) = \mathbf{C}_{\mathrm{obs}}\mathbf{x}(t) + \mathbf{D}_{\mathrm{obs}}\mathbf{u}(t) + \mathbf{v}(t) \tag{5}$$

$$\hat{\mathbf{y}}_{\mathrm{obs}}(t) = \mathbf{C}_{\mathrm{obs}}\hat{\mathbf{x}}(t) + \mathbf{D}_{\mathrm{obs}}\mathbf{u}(t) \tag{6}$$

where **x**, $\mathbf{y}_{\mathrm{obs}}$, and **v** are the state vector, sensors output, and observation noise, respectively. The notation ($\hat{}$) represents a value estimated by a Kalman filter. The coefficient matrices **A**, **B**, and **G** are derived by Eq. (1), while $\mathbf{C}_{\mathrm{obs}}$ and $\mathbf{D}_{\mathrm{obs}}$ are given based on the allocation and type of sensors.

Because LQG controllers were adopted, the gains $\mathbf{F}_{\mathrm{ctrl}}$ and $\mathbf{F}_{\mathrm{obs}}$ are given as follows:

$$\mathbf{F}_{\mathrm{ctrl}} = -\mathbf{R}^{-1}\left(\mathbf{S}^{T} + \mathbf{B}^{T}\mathbf{P}_{\mathrm{ctrl}}\right) \tag{7}$$

$$\mathbf{F}_{\mathrm{obs}} = \mathbf{P}_{\mathrm{obs}}\mathbf{C}_{\mathrm{obs}}^{T}\mathbf{V}^{-1} \tag{8}$$

where $\mathbf{P}_{\mathrm{ctrl}}$ and $\mathbf{P}_{\mathrm{obs}}$ are given by the solutions of the following Riccati equations, respectively.

$$\mathbf{P}_{\mathrm{ctrl}}\left(\mathbf{A} - \mathbf{B}\mathbf{R}^{-1}\mathbf{S}^{T}\right) + \left(\mathbf{A} - \mathbf{B}\mathbf{R}^{-1}\mathbf{S}^{T}\right)^{T}\mathbf{P}_{\mathrm{ctrl}} - \mathbf{P}_{\mathrm{ctrl}}\mathbf{B}\mathbf{R}^{-1}\mathbf{B}^{T}\mathbf{P}_{\mathrm{ctrl}} + \mathbf{Q} - \mathbf{S}\mathbf{R}^{-1}\mathbf{S}^{T} = \mathbf{O} \tag{9}$$

$$\mathbf{A}\mathbf{P}_{\mathrm{obs}} + \mathbf{P}_{\mathrm{obs}}\mathbf{A}^{T} - \mathbf{P}_{\mathrm{obs}}\mathbf{C}_{\mathrm{obs}}^{T}\mathbf{V}^{-1}\mathbf{C}_{\mathrm{obs}}\mathbf{P}_{\mathrm{obs}} + \mathbf{G}\mathbf{W}\mathbf{G}^{T} = \mathbf{O} \tag{10}$$

In Eq. (10), the matrices **V** and **W** are the power spectrum density of the observation noise and ground motion, respectively. In Eq. (9), the matrices **Q**, **S**, and **R** are those in the following cost function (J), which is minimized by the LQG controller:

$$J = \mathrm{E}[\mathbf{y}_{\mathrm{ctrl}}^{T}(t)\,\mathbf{y}_{\mathrm{ctrl}}(t) + \mathbf{u}^{T}(t)\,\mathbf{R}\,\mathbf{u}(t)] = \mathrm{E}[\mathbf{x}^{T}(t)\,\mathbf{Q}\,\mathbf{x}(t) + 2\mathbf{x}^{T}(t)\,\mathbf{S}\mathbf{u}(t) + \mathbf{u}^{T}(t)\,\mathbf{R}\,\mathbf{u}(t)] \qquad (11)$$

where the output vector ($\mathbf{y}_{\mathrm{ctrl}}$) is given by

$$\mathbf{y}_{\mathrm{ctrl}}(t) = \mathbf{C}_{\mathrm{ctrl}}\mathbf{x}(t) + \mathbf{D}_{\mathrm{ctrl}}\mathbf{u}(t) \qquad (12)$$

and the matrices $\mathbf{C}_{\mathrm{ctrl}}$ and $\mathbf{D}_{\mathrm{ctrl}}$ are selectively given based on control objectives, i.e., objective responses to be suppressed by the controllers. The absolute acceleration of building layers was chosen for suppression of the building response and the drift of the isolation device was chosen for suppression of the server response.

3. DESIGN SCHEME OF CONTROL PARAMETERS

In this study, two cost function terms for the building and computer server responses were combined using a weighting factor α and $(1 - \alpha)$. When $\alpha = 0$, the cost function contains only the building response term and the controller primarily aims to suppress the building response. When $\alpha = 1$, the computer server is the primary response. In Eq. (11), the diagonal matrix **R** consists of weighting parameters R_b for the building AMD and R_s for the semi-active damper for the server. Thus, there are three weighting parameters to be determined: α, R_b, and R_s.

For this parameter design, the scheme shown in Fig. 1 is proposed. The R_b value is determined first because the acceleration response of a building tends to be large, as discussed later in Section 4. Then, the R_s value is selected considering the trade-off relation between the isolation device drift and server acceleration. Finally, the α value is selected so that the objective responses are less than the threshold values.

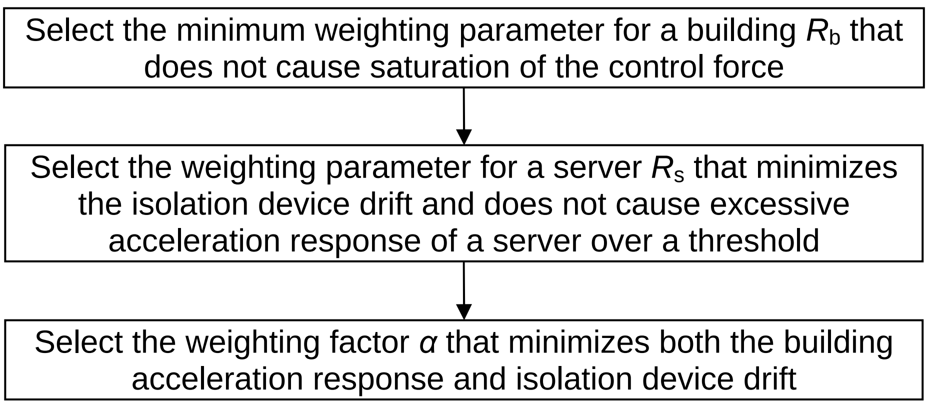

Fig. 1 Flow chart to design control parameters

4. CASE STUDY

4.1 Model of target system

The target system is a 15-story data center, which accommodates a server with an isolation device placed on the 9th floor. Table 1 lists the model parameters of the target system.

Table 1 Model parameters

Component	Parameter	Value
Building	Number of stories	15
	Mass of each layer	1×10^6 kg
	Story height	5 m
	Fundamental period	2 s
	Damping factor of 1st mode	0.02
AMD for Building	Installed location	15th layer mass (top)
	Maximum force	300 kN
Server computer	Placed location	8th layer mass (9th floor)
	Mass	400 kg
	Natural period	0.3 s
	damping factor	0.01
Isolation device	Mass	50 kg
	Natural period	3.5 s
	damping factor	0.50
Semi-active oil damper for isolation device	Minimum damping coefficient	30 Ns/m
	Maximum damping coefficient	300 Ns/m
	Relief force	400 N
	Maximum force	500 N

The semi-active oil damper for a server can change its damping coefficient from 30 to 300 Ns/m. For the calculation of damping force, the ideal damping coefficient ($c_{\mathrm{s\_ideal}}$) is first determined by an ideal control force $u_{\mathrm{s\_ideal}}$, which is given by Eq. (3), using the following equation:

$$c_{\mathrm{s\_ideal}} = -\frac{u_{\mathrm{s\_ideal}}}{v_{\mathrm{s}}} \tag{13}$$

where v_{s} is the relative velocity at an isolation device. When $c_{\mathrm{s\_ideal}}$ is outside the range of the semi-active oil damper (30–300 Ns/m), the actual damping coefficient is set to the limit value (30 or 300 Ns/m) that is nearer to $c_{\mathrm{s\_ideal}}$. Because the damping coefficient cannot be negative, the minimum damping coefficient is determined when the signs of the control force and the relative velocity at an isolation device are the same. When the absolute value of the control force exceeds the relief force, the actual damping coefficient is set to be the minimum damping coefficient.

4.2 Analysis result

To investigate the relation between the weighting parameters and the system responses, a time-history analysis was carried out. The following four input ground motions, scaled to have peak velocities of 0.25 m/s, were inputted into the model: three records of El Centro 1940 NS, Taft 1952 EW, Hachinohe 1968 NS, and one simulated ground motion based on the “Level-1” design response spectrum prescribed by Notification No. 1461 of the Ministry of Construction, May 31, 2000, in Japan. Table 2 lists the maximum responses when the system does not have control devices.

Table 2 Maximum responses when the system does not have control devices

Response	Input ground motion			
	El Centro 1940 NS	Taft 1952 EW	Hachinohe 1968 NS	Simulated ground motion
Building acceleration [m/s^2]	4.729	5.070	3.503	1.397
Story drift angle of Building [rad]	0.004619	0.004394	0.004126	0.001604
Server acceleration [m/s^2]	1.296	0.9632	1.429	0.4315
Drift of isolation device [m]	0.2044	0.1298	0.2388	0.08376

Because the model has two control devices—the AMD for the building and the semi-active oil damper for the server—multiple control schemes were considered (Yoshida et al. 2012): centralized control, partially decentralized control, and fully decentralized control. The centralized control uses all the sensor data ($\mathbf{y}_{obs}$) to control both devices. Under partially decentralized control, the two controllers communicate and share parts of the sensor’s output data. However, under decentralized control, each controller works independently and do not communicate or share the sensor’s output data.

Fig. 2 depicts the distribution of the maximum responses under the input ground motion of the scaled El Centro record using a centralized control scheme with α = 0.5. The horizontal axes are the logarithm of the weighting parameter for the control force of the building (R_b) and the vertical axes are the logarithm of the server response (R_s). The white areas represent regions where either of the two control forces exceeded their maximum force limit, i.e., where saturation of the control force occurs.

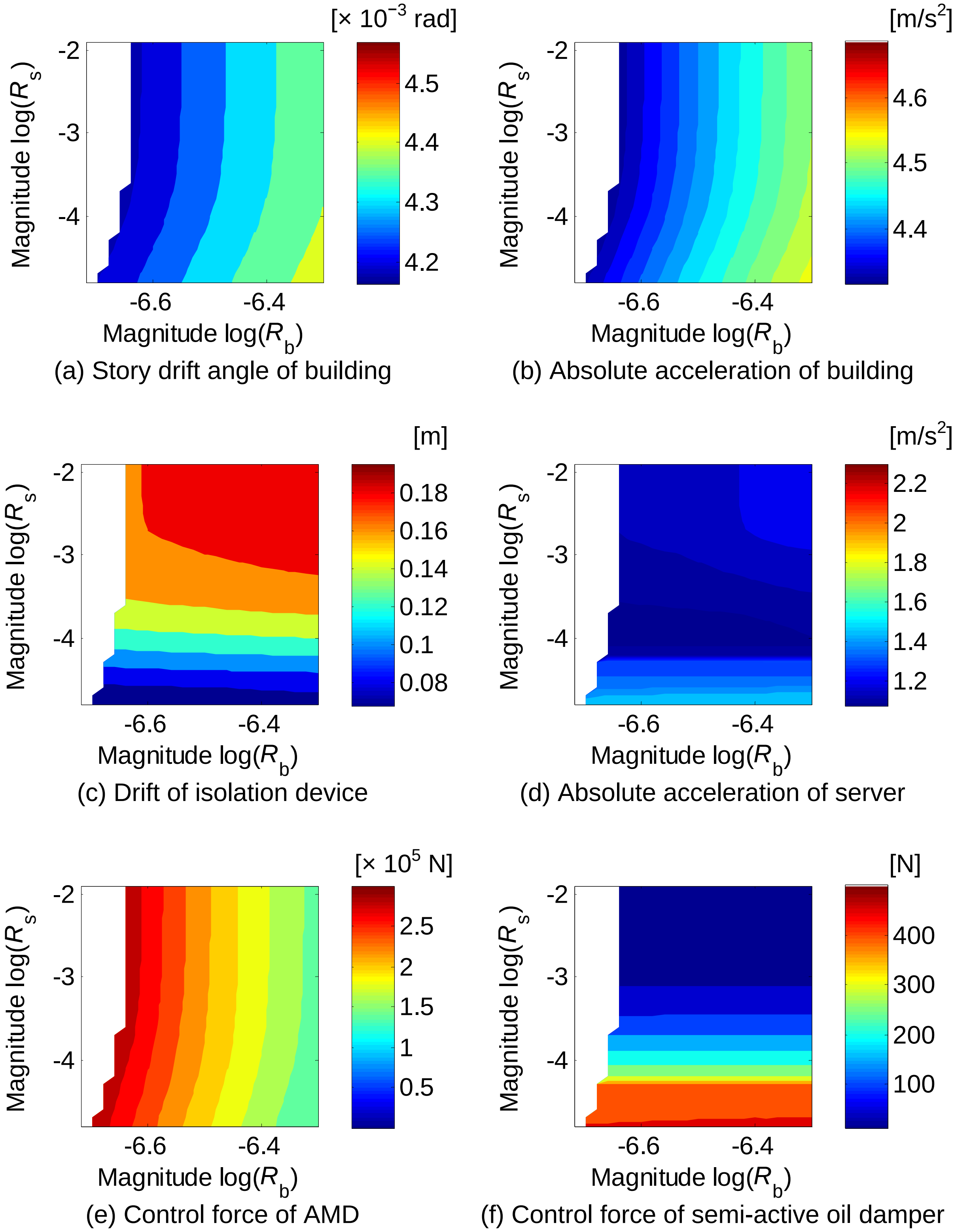

Fig. 2 Distribution of maximum response (input ground motion: El Centro, control scheme: centralized control, and α = 0.5)

It was observed that the building response decreased more when a larger control force was applied—unless the control force was not saturated. However, the server acceleration response increased when a larger control force was applied. This tendency was observed under any input ground motion, control scheme, or control objective. Thus, the validity of the proposed design scheme of control parameters was confirmed because the R_s value selected based on the scheme effectively suppressed the control objective responses.

Fig. 3 plots the normalized response–weighting factor relation, in which the maximum responses under four input ground motions are normalized by the following threshold values: 3 m/s^2 for building acceleration, 0.005 rad for story drift, 2 m/s^2 for server acceleration, and 0.2 m for drift of the isolation device. Two control objectives—the absolute acceleration of the building and the drift of the isolation device—were suppressed most effectively when the control scheme was centralized and the weighting factor α = 0.4.

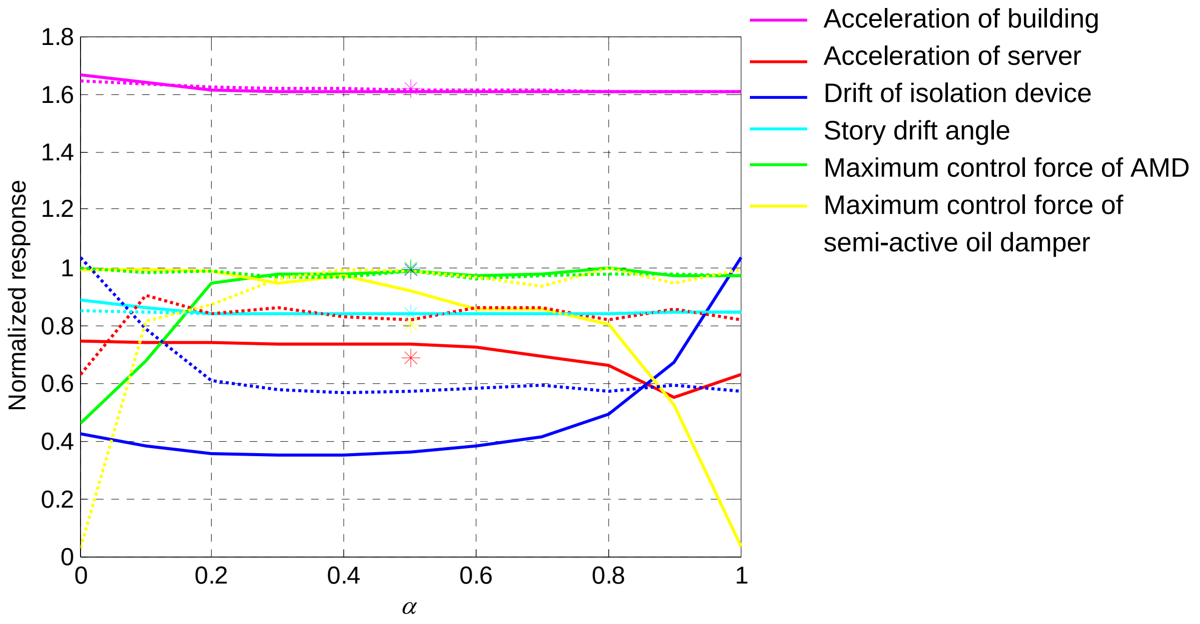

Fig. 3 Normalized response–weighting factor relation (solid line: centralized control, dotted line: partially decentralized control, and asterisk: fully decentralized control)

5. CONCLUSIONS

This study proposed a design scheme of control parameters for a building–equipment system with multiple control devices. A linear elastic model of a data center facility (a coupled system including the building and server computer) was constructed, and the evaluation function of the linear quadratic Gaussian control was formulated. Based on the dynamic analysis results, the relationship between control parameters and responses was investigated. It was verified that the proposed scheme can help in determining control parameters that can properly suppress the objective responses considering the capacity of control devices and efficiency of the control forces.

ACKNOWLEDGMENTS

This research was supported by a JSPS KAKENHI Grant-in-Aid for Scientific Research (B), Grant Number 24360230.

REFERENCES

Japan Data Center Council (2012), *Verification and reconsideration of data center facility standard in light of East Japan earthquake disaster*, http://www.jdcc.or.jp/pdf/20120315JDCC_facility_standard_digest.pdf (in Japanese).

Yoshida, M., Kohiyama, M., and Takahashi, M. (2012), "Comparative study between centralized and decentralized LQR controls of a building-elevator system," *Proceedings of 15th World Conference on Earthquake Engineering*, Lisbon, Portugal, Paper No. 2819, 10 pp.